THE PENNSYLVANIA STATE UNIVERSITY
SCHREYER HONORS COLLEGE

DEPARTMENT OF
MECHANICAL AND NUCLEAR ENGINEERING

DETERMINATION OF THE NATURAL FREQUENCIES OF MONOLAYER GRAPHENE

CAMERON S. NELSON
SPRING 2014

A thesis
submitted in partial fulfillment
of the requirements
for a baccalaureate degree
in Mechanical Engineering
with honors in
Mechanical Engineering

Reviewed and approved* by the following:

Alok Sinha
Professor of Mechanical Engineering
Co-Thesis Supervisor

Mauricio Terrones
Professor of Physics and Material Science and Engineering
Co-Thesis Supervisor

Domenic Santavicca
Professor of Mechanical Engineering
Honors Adviser

* Signatures are on file in the Schreyer Honors College.

ABSTRACT

The determination of the natural frequencies of graphene is conducted in this thesis by both theoretical and experimental approaches. The theoretical determination involves using classical mechanics with a hierarchical progression whereby complexity of the analysis is elevated from linear to square to hexagonal lattices. The experimental determination of natural frequencies begins with procedures for the synthesis of graphene and then describes how the Raman microscope develops a plot of the Raman spectrum. Upon closer observation of the G-band of the Raman spectrum, the experimental natural frequency is determined, and then compared with the theoretical natural frequency. Last, possible errors of the theoretical analysis and ideas that could be implemented to improve the theoretical result are discussed.

TABLE OF CONTENTS

LIST OF FIGURES

ACKNOWLEDGEMENTS

I am thankful for the opportunity to attend Penn State, which was made possible by my family, specifically, my dad and mom, Andrew and Paula Nelson, and my grandpa, Stuart Nelson.

Throughout the completion of this thesis, I had lots of help from my thesis advisors, Dr. Alok Sinha and Dr. Mauricio Terrones, my honors advisor, Dr. Domenic Santavicca, and lab assistants, Anupama Ghosh and Simin Feng. Thank you.

Chapter 1

Introduction

The interest of this thesis is in the determination of the natural frequencies of a monolayer sheet of graphene. Graphene consists of carbon atoms arranged in a hexagonal lattice. Therefore, this thesis will begin with some background information on both carbon and pure carbon structures.

Carbon (C) is a nonmetallic element, found in group fourteen on the periodic table, has an atomic number of six. It consists of six protons, six neutrons, and six electrons in its most stable form giving it an atomic weight of 12.0107 g/mol. Carbon's melting and boiling points are approximately $3{,}550^0$C (6,421°F) and $4{,}287^0$C (7,748 °F) respectively. In nature, carbon is present in pure forms such as diamond or graphite, as well as impure forms such as coal, charcoal, and soot [1].

Carbon has six electrons; two in the 1s orbital, two in the 2s orbital, and two in the 2p orbital. The two 1s electrons, also called core electrons, are very tightly bound to the nucleus with an ionization energy of -285 eV and do not partake in bonding with other atoms. The energy difference between the 2s and 2p orbitals is less than the energy gained by carbon-carbon bonding, therefore allowing carbon to create hybridized orbitals, which share electrons. When carbon is bonded in a linear chain, known as polyene, it forms two sp hybridized orbitals with one 2s and one 2p orbital. Similarly, when carbon is covalently bonded with three neighboring carbons in a hexagonal (or honeycomb) lattice, known as graphene, it forms three sp^2 hybridized orbitals with one 2s and two 2p orbitals. These sp^2 hybridized orbitals are the strongest bonds found in nature with a Young's modulus on the order of 1.0 TPa (or approximately 150,000 ksi).

Last, when carbon is bonded with four carbons in a regular tetrahedron structure, known as diamond, it forms four sp^3 hybridized orbitals with one 2s and three 2p orbitals [2].

This thesis will only focus on the study of graphene. The reason for this is well stated by A. Jorio, et al. in their book *Raman Spectroscopy in Graphene Related Systems*. They state, "the delocalized electronic states in monolayer graphene are highly unusual, because they behave like relativistic Dirac fermions, that is, these states exhibit a massless-like linear energy-momentum relation (like a photon), and are responsible for unique transport (both thermal and electronic) properties at sufficiently small energy and momentum values" [2].

Graphene is classified as a nano-structure. Nanotechnology is "the application of scientific knowledge to control and utilize matter at the nanoscale, where size related properties and phenomena can emerge (the nanoscale is the size range from approximately 1 nm to 100 nm)" as defined by the Technical Committee (TC-229) for nanotechnologies standardization of the International Organization for Standardization (ISO) [2].

Graphene refers to an atom-thick sheet of carbon atoms arranged in a hexagonal lattice structure. A single sheet of this (monolayer graphene) is denoted as 1-LG as shown in Figure 1.1. Bilayer graphene is denoted as 2-LG, three-layer graphene is denoted as 3-LG, and so on. Many layers of graphene stacked on one another is known as graphite. Graphene can be further manipulated into a variety of shapes such as ribbon, cylinders, and spheres. Carbon nanoribbon is a graphene sheet with a width of less than 100 nm and length of much greater than 100 nm. Carbon nanoribbon rolled up helically into a cylinder is known as a single-wall carbon nanotube (SWNT). Similarly, several cylinders of carbon nanotubes placed around one another are known as multi-walled carbon nanotubes (MWNT). Carbon can also be arranged into a sphere with a wall thickness of one atom. The most common example of this is the C_{60} fullerene (or "buckyball") consisting of sixty carbon atoms in a truncated icosahedron geometric arrangement. These carbon spheres are one of the smallest sp^2-sp^3 structures that can be made [2].

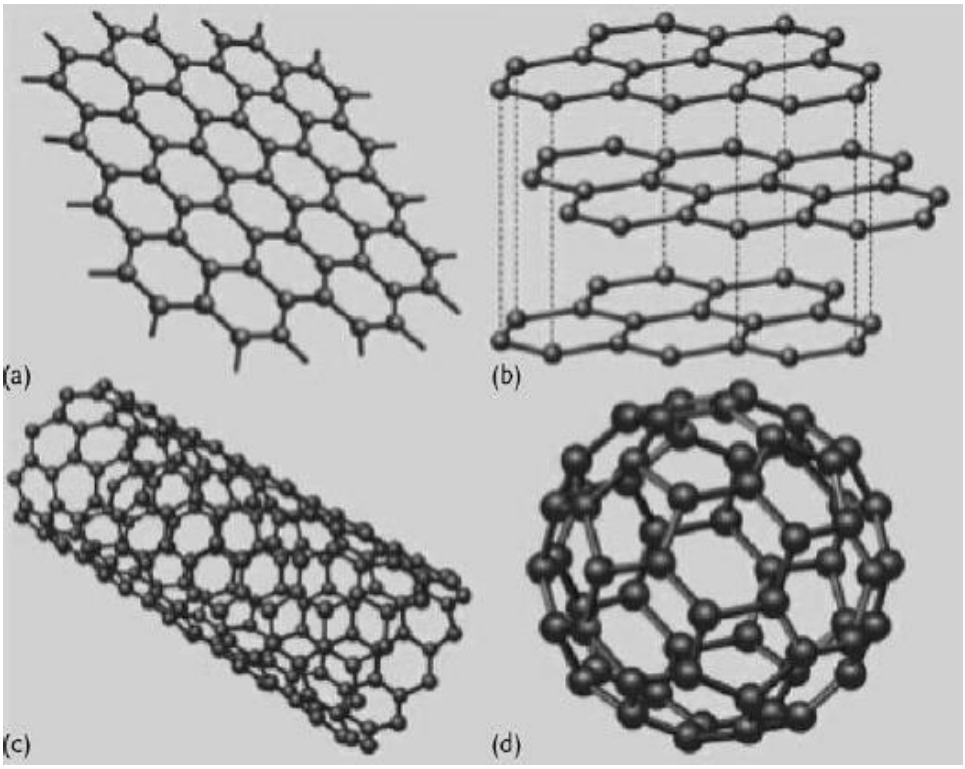

Figure 1.1: Examples of sp^2 carbon materials, including (a) single-layer graphene, (b) triple-layer graphene, (c) a single-wall carbon nanotube, and (d) a C_{60} fullerene, which includes 12 pentagons and 20 hexagons in its structure [3, 4].

This thesis focuses on determining the natural frequencies of monolayer graphene by both theoretical and experimental means. The theoretical approach will determine the natural frequency by classical mechanics, while the experimental method will use Raman spectroscopy. The interest for determining this property is due to, as mentioned above, the many uses and unique qualities of graphene. In nanotechnology, understanding the behavior and knowing the properties of nano-materials becomes important for successful design and implementation of products. As such, this thesis focuses on a fundamental property of graphene: natural frequency.

Chapter 2

Theoretical Determination of Natural Frequencies

The theoretical determination of the natural frequencies of the monolayer graphene is conducted by approaching the problem from a classical mechanics standpoint. A hierarchical approach is taken whereby the derivation of the equations of motion for a carbon structure start with a simple linear chain, then to a square lattice, and last to the complete hexagonal lattice.

Linear Chain

The free body diagram of the linear chain of identical atoms and bond stiffnesses is drawn first and the unit cell is defined as shown in Figure 2.1.

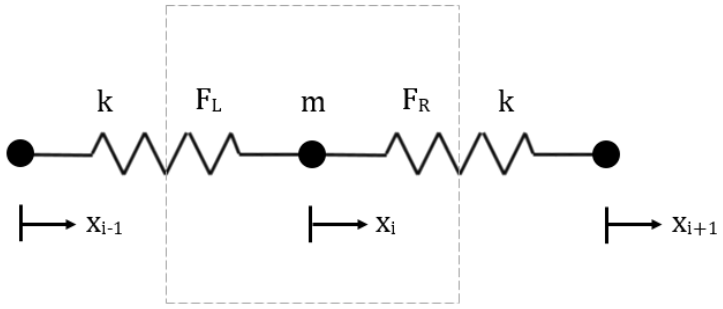

Figure 2.1: Structure of unit cell for a linear chain of identical atoms and bond stiffnesses

The equation of motion is derived for the defined unit cell as

$$\Sigma F_x = m\ddot{x}_i = F_R - F_L \tag{2.1}$$

where

$$F_R = k(x_{i+1} - x_i) \tag{2.2}$$

and

$$F_L = k(x_i - x_{i-1}) \tag{2.3}$$

Therefore, the equation of motion for the unit cell becomes

$$m\ddot{x}_i + k(-x_{i-1} + 2x_i - x_{i+1}) = 0; \quad i = 1, 2, \ldots, I \tag{2.4}$$

The matrix form of multiple equations of motions is generated as shown in Appendix A. The number of equations of motion are equivalent to the number of unit cells, I.

$$n_{EOM} = I \tag{2.5}$$

The number of unit cells is defined as 1,152 due to the fact that in a square lattice of 24 by 24 unit cells and a hexagonal lattice of 17 by 17 unit cells, each scenario will have equivalent numbers of equations of motion, 1,152. The mass of a single carbon atom is determined by taking its molar mass and dividing it by Avogadro's number.

$$m = \left(12.0107 \frac{g}{mol}\right) / \left(6.02214129e23 \frac{atoms}{mol}\right) = 1.99442e\text{-}26\ kg \tag{2.6}$$

The longitudinal stiffness of the carbon-carbon bond is approximated using the force constant parameters between carbon-carbon bonds in a hexagonal lattice, as shown in Figure 2.2.

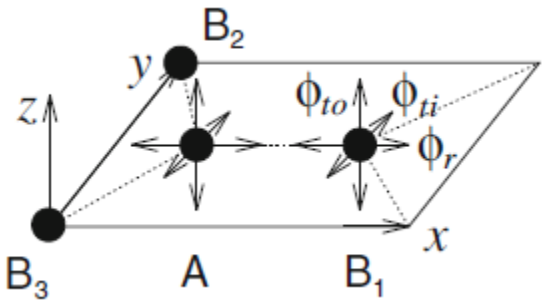

Figure 2.2: Force constants between the A and B1 atoms on a graphene sheet. Here Φ_r, Φ_{ti}, and Φ_{to} represent forces for the nearest-neighbor atoms in the radial (bond-stretching), in-plane and out-of-plane tangential (bond-bending) directions, respectively. B2 and B3 are nearest neighbors equivalent to B1, whose force constant tensors are obtained by appropriately rotating the tensor for A and B1 [5].

The values of the force constant parameters, obtained from inelastic neutron scattering measurements, are [6],

$$\Phi_r = 365.0 \frac{N}{m} \tag{2.7}$$

$$\Phi_{ti} = 245.0 \frac{N}{m} \tag{2.8}$$

$$\Phi_{to} = 98.2 \frac{N}{m} \tag{2.9}$$

An assumption is made throughout this theoretical method that the change in the direction of a given carbon-carbon bond is very small. Therefore, the stiffness of the bond is equivalent to the nearest-neighbor in the radial (bond stretching) direction force constant.

$$k = 365.0 \frac{N}{m} \tag{2.10}$$

The mass matrix is defined as the mass of the carbon atom multiplied by an identity matrix with dimensions of n_{EOM} by n_{EOM}. Likewise, the stiffness matrix has dimensions of n_{EOM} by n_{EOM}. The stiffness matrix is now filled using the equation of motion for the linear chain starting with the unit cell i = 1, then iterating over i = 2 to I-1, and last filling in the values for unit cell i = I as shown in Appendix A. By inverting the mass matrix, multiplying it by the stiffness matrix, and then applying the eigenvalue function to it in Matlab, natural frequencies of the system are determined [7].

$$M^{-1}Kv = \omega_n{}^2 v \tag{2.11}$$

where ω_n is the natural frequency, v is the modal vector, M is the mass matrix, and K is the stiffness matrix. A histogram of the natural frequencies with bin size 1e12 rad/s is plotted, as seen in Figure 2.3, to determine the natural frequency of the entire linear chain. The theoretical natural frequency of a linear chain 1,152 unit cells in length is 2.70e14 rad/s.

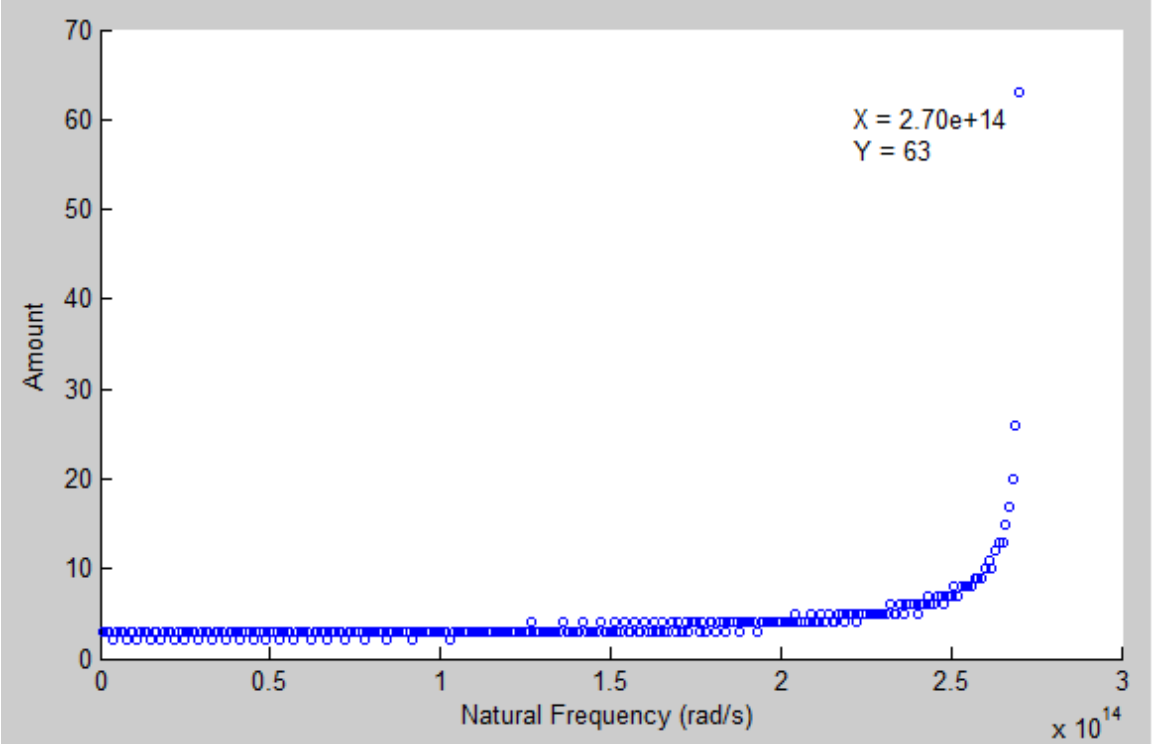

Figure 2.3: Histogram of theoretical natural frequencies for linear chain 1,152 atoms long (bin size: 1e12 rad/s)

Square Lattice

The free body diagram of the square lattice of identical atoms and bond stiffnesses is drawn first and the unit cell is defined as shown in Figure 2.4.

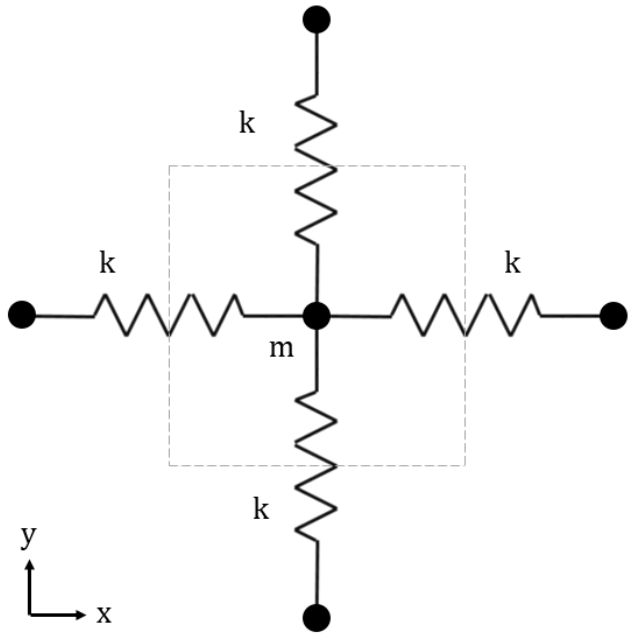

Figure 2.4: Structure of unit cell for a square lattice of identical atoms and bond stiffnesses

Taking the assumption that the motion of the atoms will keep horizontal bonds very close to 0^0 off the x-axis and vertical bonds very close to 90^0 of the x-axis, the equations of motion for the linear chain can be used for the square matrix in its x and y directions. The equations of motion for the unit cell become

$$m\ddot{x}_{i,j} + k\left(-x_{i-1,j} + 2x_{i,j} - x_{i+1,j}\right) = 0 \tag{2.12}$$

and

$$m\ddot{y}_{i,j} + k\left(-y_{i,j-1} + 2y_{i,j} - y_{i,j+1}\right) = 0 \tag{2.13}$$

where i = 1, 2, …, I and j = 1, 2, …, J.

The matrix form of multiple equations of motion is generated as shown in Appendix B. The number of equations of motion is defined as,

$$n_{EOM} = 2IJ \tag{2.14}$$

The number of unit cells is defined as 24 by 24 due to the fact that the number of equations of motion generated is equivalent to the number for a hexagonal lattice of 17 by 17 unit cells. The

mass and stiffness values used are equivalent to the linear case. Similarly, the mass and stiffness matrix are generated with dimensions of n_{EOM} by n_{EOM}. Due to the previously stated assumption that the direction of bonds changes very little, the square lattice in essence turns into the I plus J linear chains. Therefore, the generation of the stiffness matrix is identical to 48 identical linear chains with 24 unit cells in each linear chain. See Appendix B for the iteration code. Like the linear system, a histogram is plotted showing the natural frequencies of the square lattice as shown in Figure 2.5.

The 24 by 24 square lattice yields a theoretical natural frequency of 2.65e14 rad/s. It is important to recognize that the square lattice was modelled as many linear chains. Therefore the system is only as good as the amount of equations of motion in an individual linear chain and then that system is repeated over and over again. That is why the amounts of natural frequencies in given bins are multiples of an integer value, 48. If the square lattice was modelled with a much larger square lattice, it would yield the exact same curve and peak as the linear system above.

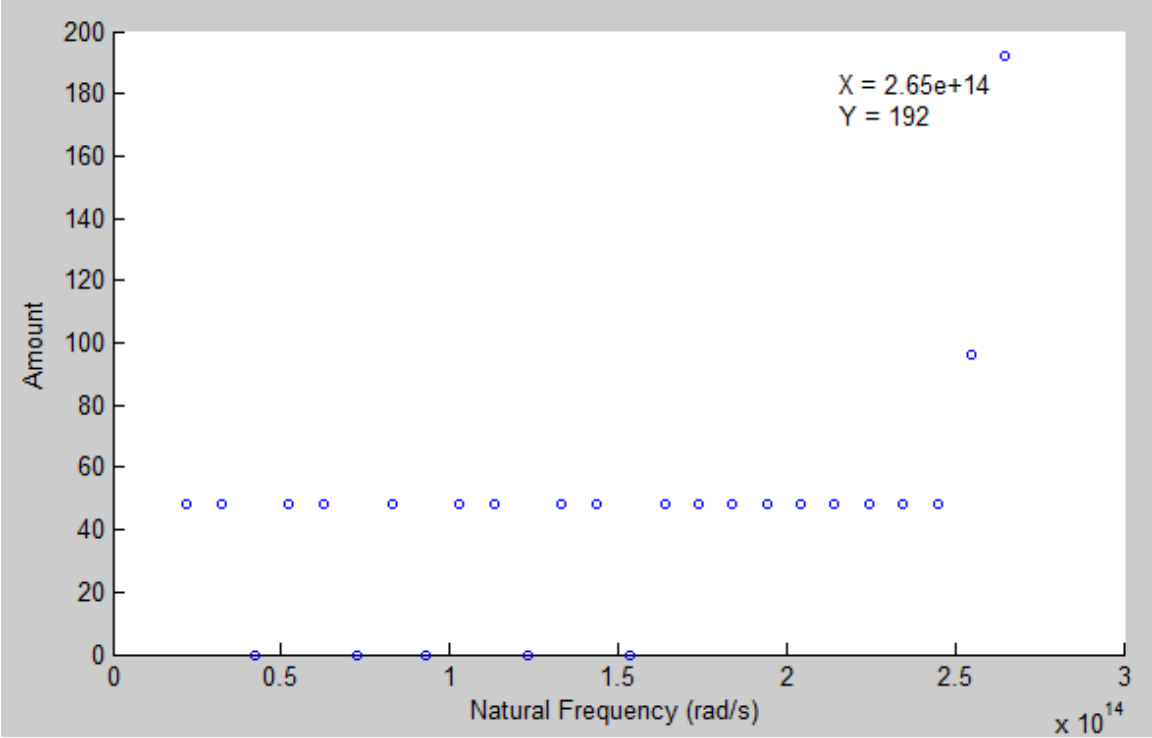

Figure 2.5: Histogram of theoretical natural frequencies for 24 by 24 square lattice (bin size: 1e13 rad/s)

Hexagonal Lattice

The unit cell of the hexagonal lattice of identical atoms and bond stiffnesses is determined first as shown in Figures 2.6. The unit cell is in the shape of a diamond and consists of two atoms arbitrarily defined as atom A (upper atom) and atom B (lower atom). If a given cell is defined as (i, j), then the cell to its upper right is (i+1, j), and the cell to its upper left is (i, j+1) also shown in Figure 2.6.

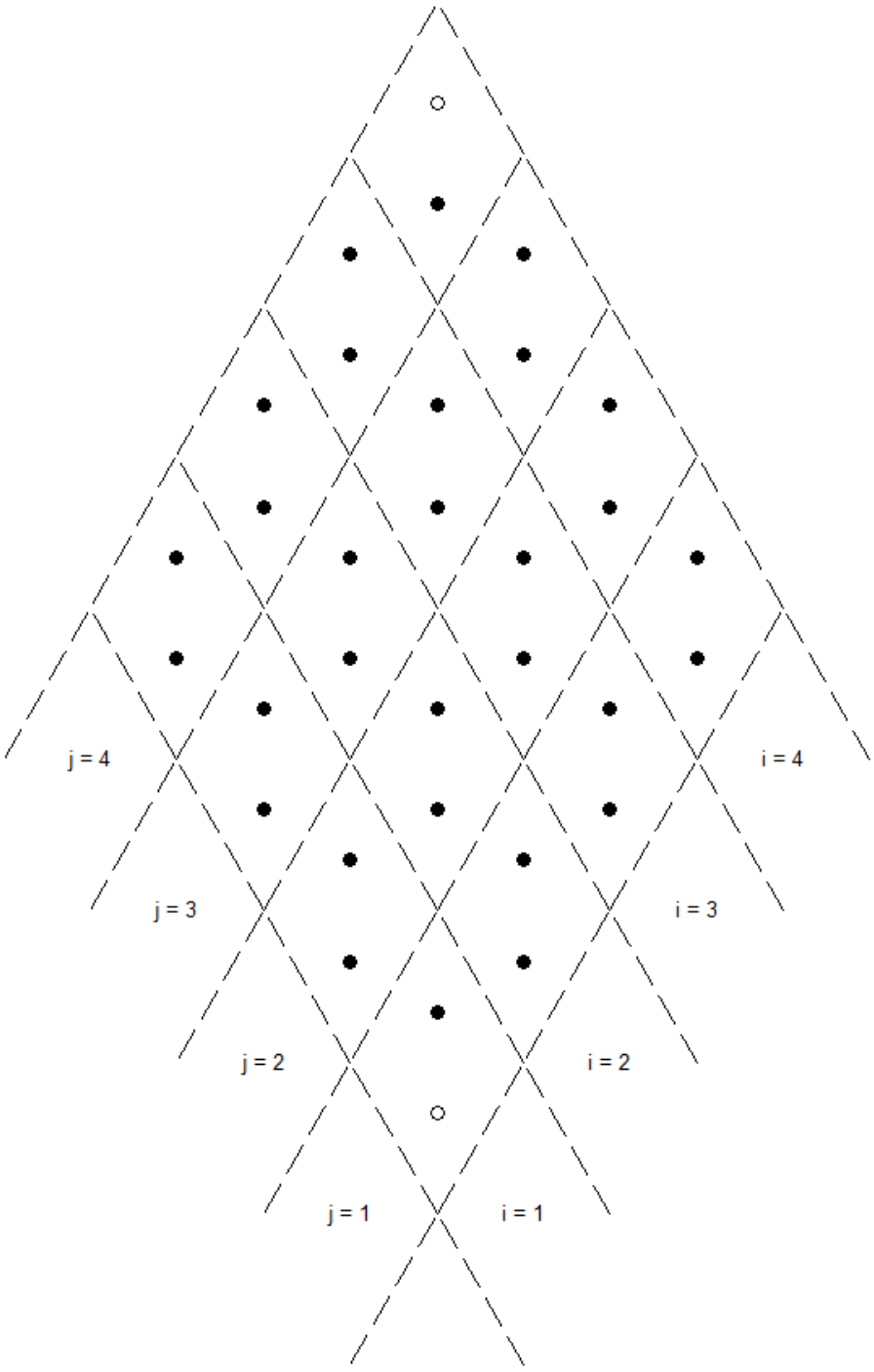

Figure 2.6: Hexagonal lattice with unit cells in the shape of diamonds

Next the structure of the unit cell is drawn as shown in Figure 2.7.

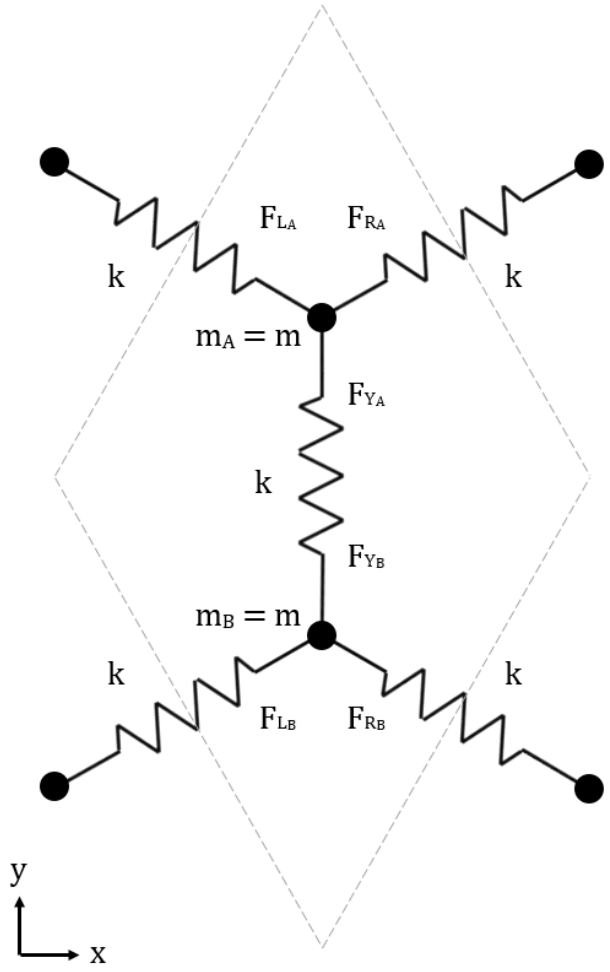

Figure 2.7: Structure of unit cell for a hexagonal lattice of identical atoms and bond stiffnesses

Equations of motion can now be determined with the assumption that the variance of the angles of the hexagonal lattice bonds is very small as the atoms move. The equations of motion are

$$\Sigma F_{x_A} = m\ddot{x}_{A_{i,j}} = \frac{\sqrt{3}}{2}F_{R_A} - \frac{\sqrt{3}}{2}F_{L_A} \tag{2.15}$$

$$\Sigma F_{y_A} = m\ddot{y}_{A_{i,j}} = \frac{1}{2}F_{R_A} + \frac{1}{2}F_{L_A} - F_{Y_A} \tag{2.16}$$

$$\Sigma F_{x_B} = m\ddot{x}_{B_{i,j}} = \frac{\sqrt{3}}{2}F_{R_B} - \frac{\sqrt{3}}{2}F_{L_B} \tag{2.17}$$

$$\Sigma F_{y_B} = m\ddot{y}_{B_{i,j}} = -\frac{1}{2}F_{R_B} - \frac{1}{2}F_{L_B} + F_{Y_B} \tag{2.18}$$

Similar to the linear and square lattices, the force contributed by a bond is proportional to its change in length by its spring constant, k. The determination of the change in length (δ) of the A atom's upper-right bond begins with defining the motion of the A atom and the B atom of the unit cell to the upper-right of the given unit cell. The problem is simplified by fixing the B-atom and allowing the A atom to move in the x-direction by $x_A - x_B$ and in the y-direction by $y_A - y_B$ as shown in Figure 2.8.

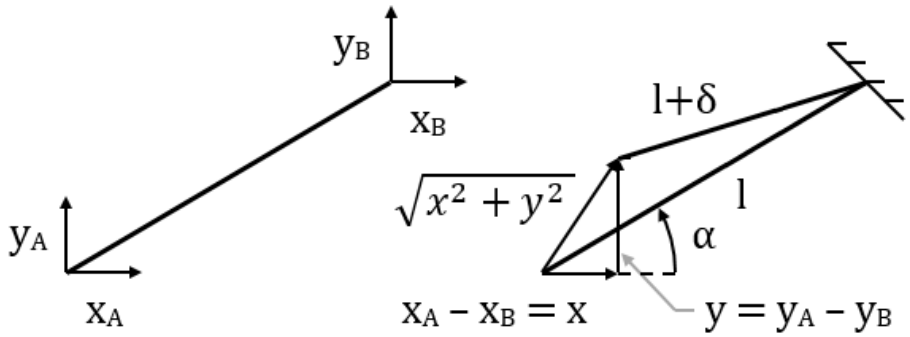

Figure 2.8: Drawing showing the change in the length (δ) of the bond when its ends move

Using the algebraically determined lengths of the triangle formed by the movement of the lower-left point in the above diagram and the law of cosines the following is determined.

$$\cos\left(tan^{-1}\left(\frac{y}{x}\right) - \alpha\right) = \frac{l^2+(x^2+y^2)-(l+\delta)^2}{2l\sqrt{x^2+y^2}} \tag{2.19}$$

After some algebra, the equation becomes

$$(l + \delta)^2 = l^2\left[1 + \frac{x^2+y^2}{l^2} - \frac{2x\cos\alpha}{l} - \frac{2y\sin\alpha}{l}\right] \tag{2.20}$$

Making the assumption that $\frac{x}{l}$ and $\frac{y}{l}$ are very small, then $\frac{x^2+y^2}{l^2}$ is essentially zero. The equation becomes,

$$l + \delta = l\left[1 - \frac{2x\cos\alpha}{l} - \frac{2y\sin\alpha}{l}\right]^{1/2} \tag{2.21}$$

Using binomial expansion and neglecting higher order terms,

$$l + \delta \cong l\left[1 - \frac{x}{l}\cos\alpha - \frac{y}{l}\sin\alpha\right] \tag{2.22}$$

Knowing that $\alpha = \frac{\pi}{6}$, therefore,

$$\delta \cong -\frac{\sqrt{3}}{2}x - \frac{1}{2}y \tag{2.23}$$

Knowing Hooke's Law ($F = k\delta$), the forces of the five bonds in the unit cell become

$$F_{R_A} = k\left[\frac{\sqrt{3}}{2}x_{B_{i+1,j}} - \frac{\sqrt{3}}{2}x_{A_{i,j}} + \frac{1}{2}y_{B_{i+1,j}} - \frac{1}{2}y_{A_{i,j}}\right] \tag{2.24}$$

$$F_{L_A} = k\left[\frac{\sqrt{3}}{2}x_{A_{i,j}} - \frac{\sqrt{3}}{2}x_{B_{i,j+1}} + \frac{1}{2}y_{B_{i,j+1}} - \frac{1}{2}y_{A_{i,j}}\right] \tag{2.25}$$

$$F_{Y_A} = k\left[y_{A_{i,j}} - y_{B_{i,j}}\right] \tag{2.26}$$

$$F_{R_B} = k\left[\frac{\sqrt{3}}{2}x_{A_{i,j-1}} - \frac{\sqrt{3}}{2}x_{B_{i,j}} + \frac{1}{2}y_{B_{i,j}} - \frac{1}{2}y_{A_{i,j-1}}\right] \tag{2.27}$$

$$F_{R_B} = k\left[\frac{\sqrt{3}}{2}x_{B_{i,j}} - \frac{\sqrt{3}}{2}x_{A_{i-1,j}} + \frac{1}{2}y_{B_{i,j}} - \frac{1}{2}y_{A_{i-1,j}}\right] \tag{2.28}$$

$$F_{Y_B} = k\left[y_{A_{i,j}} - y_{B_{i,j}}\right] \tag{2.29}$$

Therefore, the equations of motion for the unit cell become

$$m\ddot{x}_{A_{i,j}} + \frac{k}{4}\left[6x_{A_{i,j}} - 3x_{B_{i,j+1}} + \sqrt{3}y_{B_{i,j+1}} - 3x_{B_{i+1,j}} - y_{B_{i+1,j}}\right] = 0 \tag{2.30}$$

$$m\ddot{y}_{A_{i,j}} + \frac{k}{4}\left[6y_{A_{i,j}} - 4y_{B_{i,j}} + \sqrt{3}x_{B_{i,j+1}} - y_{B_{i,j+1}} - \sqrt{3}x_{B_{i+1,j}} - y_{B_{i+1,j}}\right] = 0 \tag{2.31}$$

$$m\ddot{x}_{B_{i,j}} + \frac{k}{4}\left[-3x_{A_{i-1,j}} - \sqrt{3}y_{A_{i-1,j}} - 3x_{A_{i,j-1}} + \sqrt{3}y_{A_{i,j-1}} + 6x_{B_{i,j}}\right] = 0 \tag{2.32}$$

$$m\ddot{y}_{B_{i,j}} + \frac{k}{4}\left[-\sqrt{3}x_{A_{i-1,j}} - y_{A_{i-1,j}} + \sqrt{3}x_{A_{i,j-1}} - y_{A_{i,j-1}} - 4y_{A_{i,j}} + 6x_{B_{i,j}}\right] = 0 \tag{2.33}$$

where i = 1, 2, …, I and j = 1, 2, …, J.

The matrix form of multiple equations of motion is generated as shown in Appendix C. In order to generate the mass and stiffness matrices a lattice is considered having i = I by j = J unit cells where I = J such as is shown in Figure 2.6. The lower most atom and the upper most atom of the I by J lattice are not included as moving atoms. Therefore, the number of equations of motion is

$$n_{EOM} = 4IJ - 4 \tag{2.34}$$

The size of the lattice is defined as 17 by 17 for the reasons mentioned in the linear chain and square lattice sections. The mass and stiffness values used are equivalent to the linear case. Mass and stiffness matrices are generated, however, the stiffness matrix is much more difficult to fill, and involves splitting up the I by J lattice into nine pieces. See Appendix C, while referring to Figure 2.6, for more details on how the stiffness matrix is generated. The code last plots a histogram of the natural frequencies as shown in Figure 2.9. The 17 by 17 hexagonal lattice yields a theoretical natural frequency of 2.34e14 rad/s, which corresponds to the G-band natural frequency of graphene described in Chapter 3.

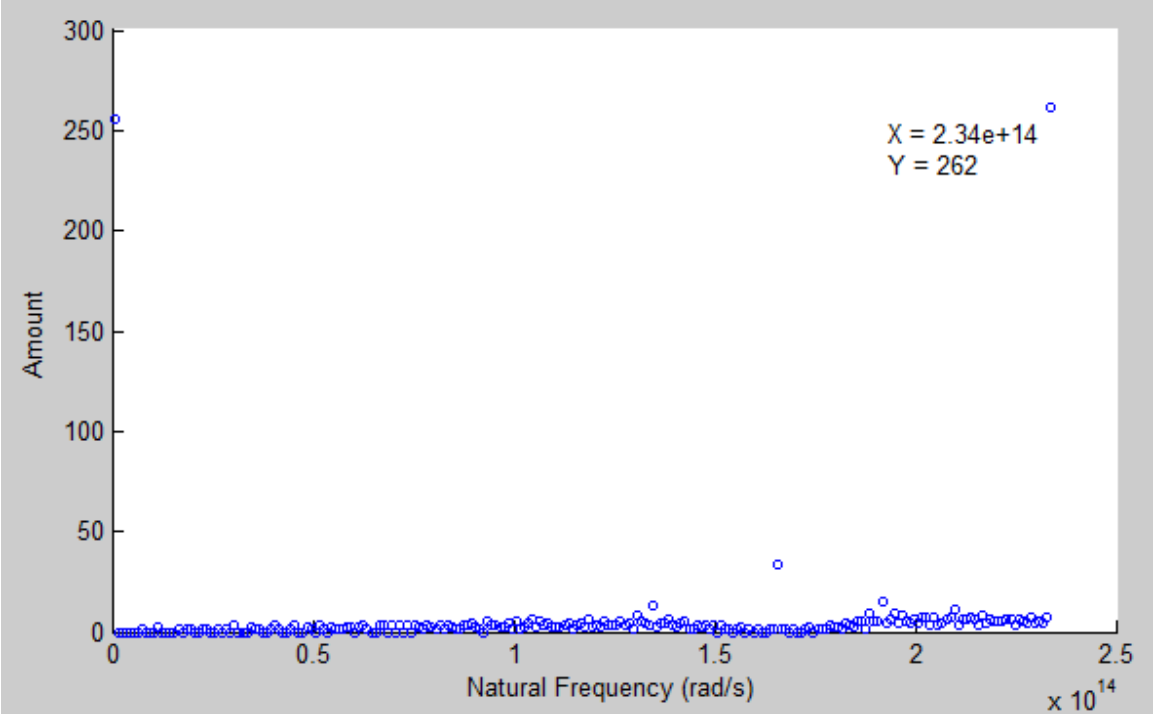

Figure 2.9: Histogram of theoretical natural frequencies for 17 by 17 hexagonal lattice (bin size: 1e12 rad/s)

Chapter 3

Experimental Determination of Natural Frequencies

The experimental approach, to determine the natural frequencies of monolayer graphene, involves first, the synthesis of graphene and second, its experimentation by Raman spectroscopy.

Overview: In order to synthesize graphene, hexane is used as a source of carbon. In order to free the carbon atoms from the hexane, it must be dissociated in a furnace at high temperatures. Once the hexane is dissociated, carbon atoms try to rearrange themselves into a stable form. A solid surface allows for the carbon to form into a stable two-dimensional structure, monolayer graphene. A piece of copper foil is ideal for this for two reasons: 1) It dissolves carbon at high temperatures and 2) acts as a catalyst for this reaction [8].

Procedure: An approximately 2 cm by 2 cm piece 99.8% pure copper foil with 0.025 mm thickness is dipped in 1:3 vol/vol HCl/H_2O for 5-10 seconds and then is washed thoroughly in DI water and dried with nitrogen gun. Then it is placed on a quartz slide and inserted into a 1.5 inch diameter quartz tube 4 ft long, which is placed into a furnace as shown in Figures 3.1 and 3.2. Next, the system is purged with a mixture of argon and hydrogen, blown through the quartz tube at rates of 755 sccm (standard cubic cm/min) and 45 sccm respectively for twenty minutes. The temperature of the furnace is now raised from approximately 25^0C to 1000^0C in an interval of fifty minutes. The temperature profile progresses first from 25^0C to 100^0C in three minutes, then remains at 100^0C for ten minutes to allow oxygen and moisture trapped on the surface of the copper foil to escape. Next, the temperature is raised to 200^0C in three minutes and kept there for ten minutes to allow low-temperature annealing. Last, the temperature is raised to 1000^0C in twenty-four minutes. (Figure 3.3) Copper melts at $1{,}083^0$C, so the maximum temperature of the system should stay well below that. After reaching 1000^0C, the temperature is retained for ten minutes allowing the copper to anneal [8].

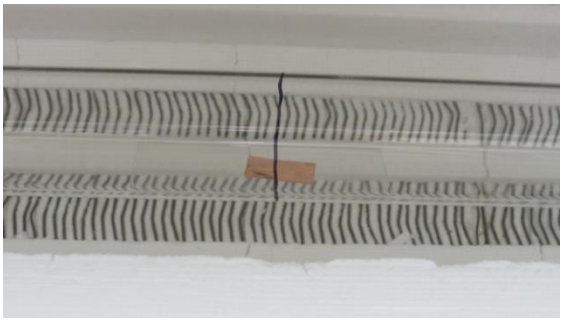

Figure 3.1: Quartz slide, placed in a quartz tube reactor

Figure 3.2: Open furnace with copper foil within

Figure 3.3: Closed furnace

Hexane, which is liquid at room temperature, is flown through metal pipe by argon, which acts as the carrier gas, at a rate of 0.1 sccm for five minutes. This then flows into the furnace through the quartz tube and then over the copper foil. At high temperatures, the hexane dissociates into smaller fragments of carbon, which dissolve onto the copper surface where islands of graphene begin to form. After five minutes, the flow of hexane is cut off and the furnace is turned off allowing the system to cool back to room temperature over approximately two hours. As the copper cools down, it gives off dissolved carbon as the graphene continues to form. Any amorphous carbon, if generated in the process, is cleaned off by the hydrogen which continues to flow over the copper surface. This also helps in greatly reducing imperfections present in the graphene. Once the system reaches room temperature, the quartz slide, containing the copper foil, containing the graphene, can be removed [8].

Graphene on copper foil gives poor results during Raman spectroscopy due to the fact that copper interferes with the Raman scattering. Therefore, it is necessary to transfer the graphene sheet to another substrate. In order to remove the copper, the copper foil, containing the graphene, is taped to a smaller, square-shaped glass slide as shown in Figure 3.4. Next, 5-10 μL of PMMA (Polymethyl mathacrylate) is dropped onto it and spin coated for one minute at a speed of 4,000 rpm allowing the PMMA to distribute evenly over the graphene. Following this, the copper foil is un-taped from the slide and placed carefully on the top of a bath of copper etchant (iron (III) chloride and hydrochloric acid) at 50^0C as shown in Figure 3.5. Copper etchant dissolves the copper in approximately twenty minutes, removing it from the graphene and PMMA forming copper (II) chloride and iron (II) chloride in aqueous solution as shown in Figure 3.6. Next, the PMMA coated graphene is fished out using a 300 nm silicon oxide/silicon wafer as shown in Figure 3.7. The wafer, containing graphene/PMMA is now rinsed with DI water twice and allowed to dry for one hour. Lastly, the PMMA is removed from the graphene by rinsing the wafer in acetone and isopropanol alcohol for ten seconds each repeatedly back and forth for two minutes as shown in Figure 3.8. After rinsing, the graphene, visible because of the contrast change on 300 nm SiO_2/Si wafer, is now ready for testing. (Figure 3.9) This concludes the process of synthesis of monolayer graphene [8].

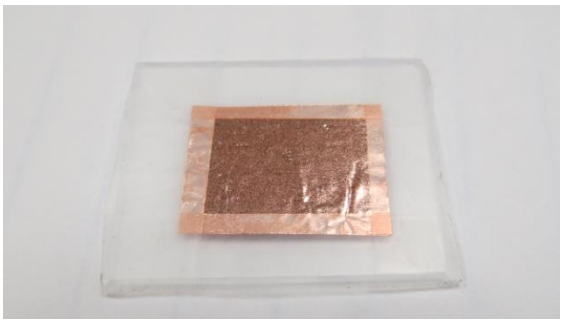

Figure 3.4: Graphene on copper foil, taped on a glass slide

Figure 3.5: Copper foil floating on copper etchant

Figure 3.6: Copper foil dissolving in copper etchant

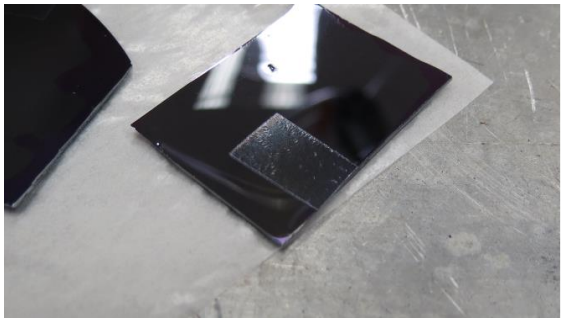

Figure 3.7: PMMA coater graphene on 300 nm SiO_2/Si wafer

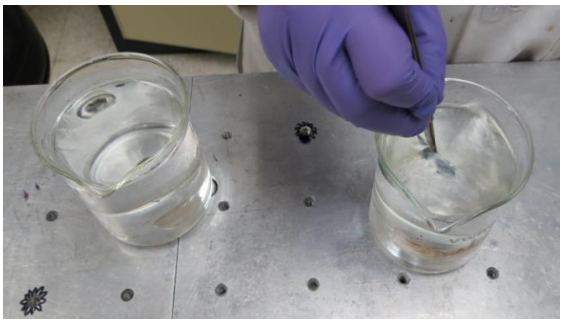

Figure 3.8: Removal of PMMA in acetone and IPA

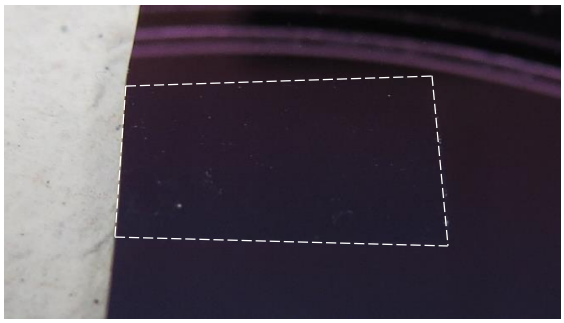

Figure 3.9: Graphene on 300 nm SiO_2/Si wafer

The natural frequencies of monolayer graphene can be determined by conducting a Raman spectroscopy experiment on the graphene sample. To do this, a 514 nm (green) laser is shot at the graphene by a Raman microscope as shown in Figures 3.10 and 3.11.

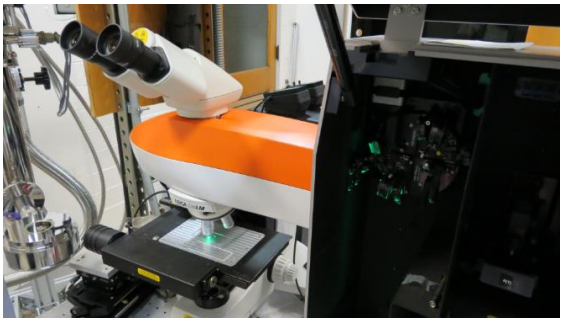

Figure 3.10: Raman microscope

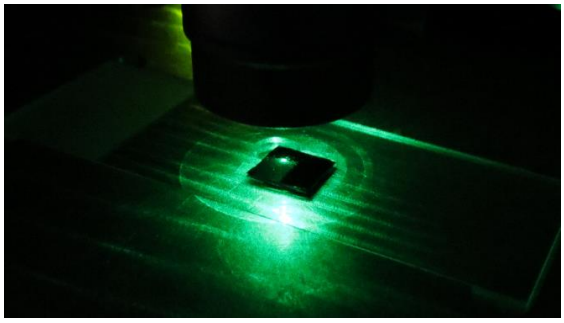

Figure 3.11: Graphene being shot with 514 nm laser

Simin Feng, a graduate student at Penn State working with graphene, describes that, "the interaction (usually inelastic scattering) between the laser photons and the material will result in

changes of the photon energies, thus shifting the wavelength of emitted photons [9]". This shift in emitted photon wavelength is called the Raman shift. A sensor counts the number of photons per time, and then a computer interprets the data and plots a trace of the Raman shift, where each data point represents the amount of Raman shift values within a set range around the x-position point (Figure 3.12) [9].

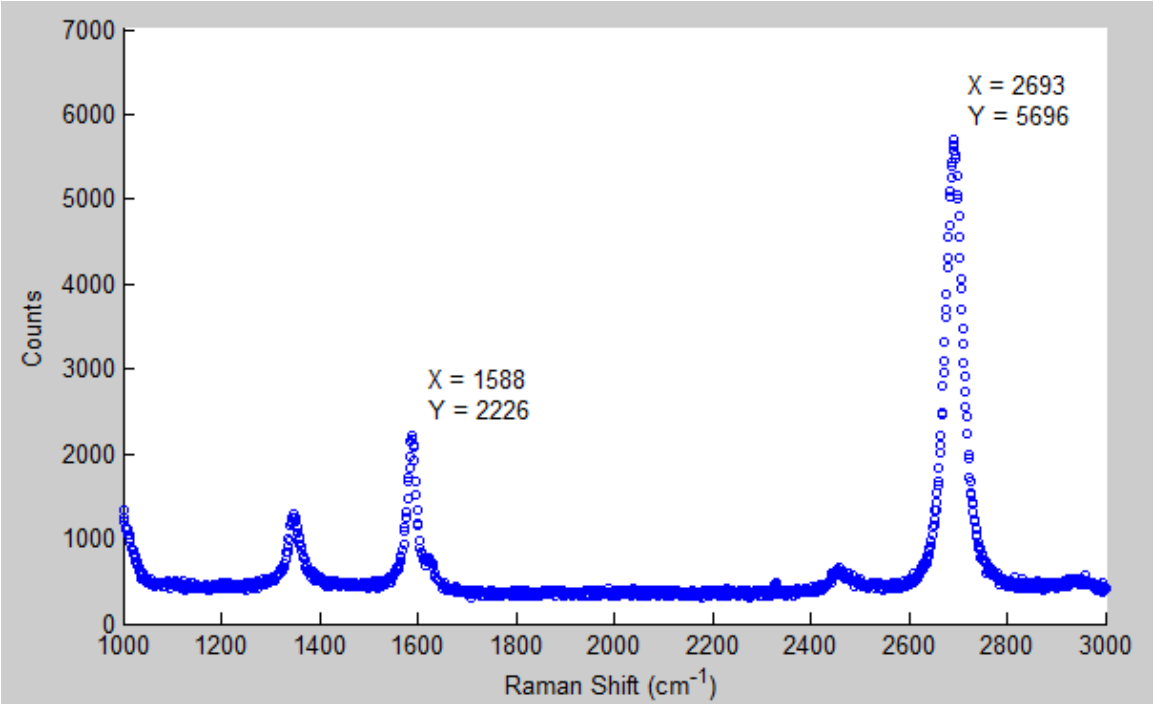

Figure 3.12: Raman spectrum of a graphene sample, shown in Figure 3.11

The peak values on this plot from left-to-right represent the natural frequencies of the D, G, D', and G' bands as also shown in Figure 3.13.

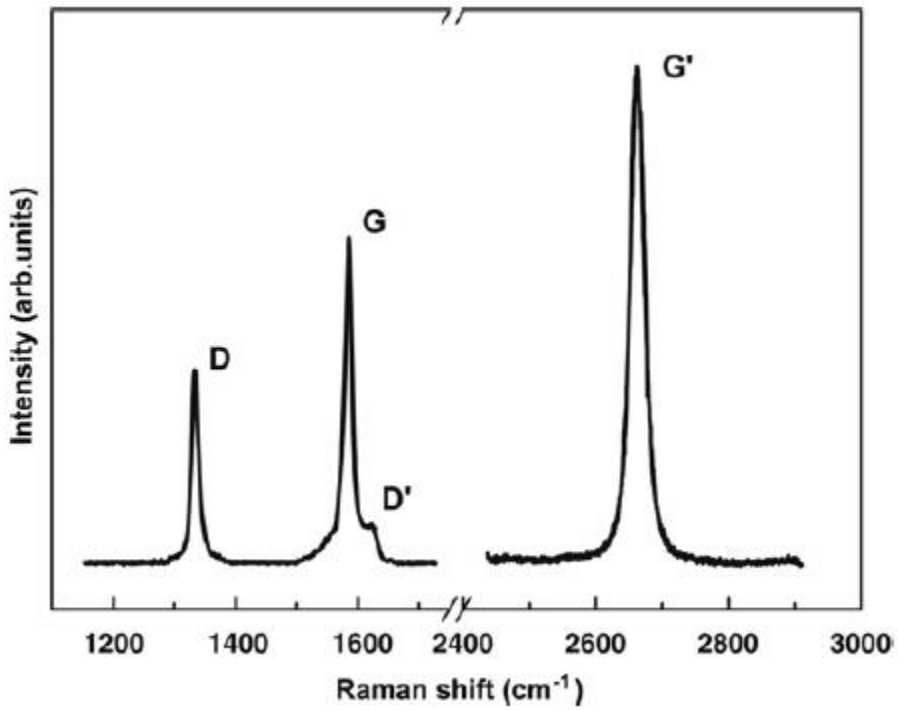

Figure 3.13: Raman spectrum of a graphene edge, showing the main Raman features, the D, G and G' bands taken with a laser excitation energy of 2.41 eV [10].

The D and D' bands show that there is some defects in the graphene, while the G and G' bands represent the natural frequencies of perfect monolayer graphene [9]. Analyzing the experimental plot, yields a G and G' band Raman shift values of 1,588 cm^{-1} and 2,693 cm^{-1} respectively. These values are converted to natural frequencies by the equation,

$$\omega_n = 2\pi\bar{\nu}c \tag{3.1}$$

where ω_n is the natural frequency, $\bar{\nu}$ is the spectroscopic wavenumber (Raman shift), and c is the speed of light, 2.99792458e8 m/s. The experimental natural frequencies of the graphene become,

$$\omega_{n_G} = 2.991e14\ rad/s \tag{3.2}$$

$$\omega_{n_{G'}} = 5.073e14\ rad/s \tag{3.3}$$

Chapter 4

Summary and Conclusion

The experimental analysis yielded a G-band natural frequency of 2.991e14 rad/s. Comparing Figures 3.12 and 3.13, the experimental value of the G-band Raman shift is in the correct range, 1580 to 1590 cm^{-1}. Therefore the calculated value of the G-band natural frequency is very trustworthy.

Comparing the experimental natural frequency with the theoretical natural frequency for graphene, 2.34e14 rad/s, yields a percent error of 21.8%. Causes for the theoretical error would be that the complex carbon-carbon bonds within the hexagonal lattice were modelled as linear springs with resistance only in the longitudinal direction. Also, there was no differentiation between carbon-carbon single and double bonds. Furthermore, the change in the direction of these bonds was considered very small. The atoms were also not allowed to move in the direction normal to the graphene sheet. For these reasons, the theoretical model yielded one natural frequency for the graphene lattice, which had a 21.8% error to the experimental value.

The theoretical determination of the natural frequency of graphene is effective at determining the G-band natural frequency close to the experimental value. There is some error, and to properly understand the natural frequency of the structure it would be important to experimentally determine that value with for example Raman spectroscopy. The theoretical analysis could be improved by modelling the bond with its bond-bending stiffness values while allowing the system to move normal to the plane of graphene. In addition, differentiating between single and double bonds may yield better results.

Appendix A

Linear Chain Matlab code

```
% Cameron S. Nelson
% Schreyer Honors College Thesis on Graphene

clear all
close all
clc

%                DETERMINATION OF NATURAL FREQUENCIES FOR
%                      LINEAR CHAIN OF CARBON ATOMS


% Size of Lattice
I       = 1152;                         % Number of Unit Cells
n_EOM   = I;                            % Number of Equations of Motion

% Mass (kg)
m = 12.0107/6.02214129e23/1000;         % Mass of a Carbon Atom

% Force Constant Parameters for 2D Graphene (N/m) [6]
Phi_r_1 = 365.0;                        % Radial
Phi_ti1 = 245.0;                        % Transverse in-plane
Phi_to1 =  98.2;                        % Transverse out-of-plane

k       = Phi_r_1;                      % Bond Longitudinal Stiffness

% Mass and Stiffness Matrices for Lattice
M       = m*eye(n_EOM);                 % Mass Matrix
S       = zeros(n_EOM);                 % Stiffness Matrix (divided by k)

% Iteration to fill Stiffness Matrix based on Equations of Motion
% i = 1
        S(1,   1        ) =  2;
        S(1,   2        ) = -1;

% i = 2 to I-1
    for a = 2: 1: I-1
        S(a, a-1        ) = -1;
        S(a, a          ) =  2;
        S(a, a+1        ) = -1;
    end

% i = I
        S(I, I-1        ) = -1;
        S(I, I          ) =  2;

K       = k*S;                          % Stiffness Matrix

% Determination of Natural Frequencies
IMK     = inv(M)*K;                     % Inverse of M times K
[V, D]  = eig(IMK);                     % V: Eigenvectors of IMK
                                        % D: Eigenvalues along diagonal
```

```
Diag    = ones(1, n_EOM);               % Diagonal to Single-Row Matrix
                                        %   Multiplier
w_n     = (Diag*D).^(1/2);              % Row Matrix of Natural Frequencies

% Natural Frequencies Histogram
width = 1e12;                           % Approximate width of Bins
Bins = floor((max(w_n)-min(w_n))/width);% Number of Bins
Width = (max(w_n)-min(w_n))/Bins;       % Actual width of Bins

v = 0;
BinCenters = zeros(1, Bins);            % Centerpoint of Bins Matrix
for w = min(w_n)+Width/2: Width: max(w_n)-Width/2
    v = v+1;
    BinCenters(1, v) = w;               % Centerpoint for Individual Bin
end

N = hist(w_n, Bins);                    % Number of Nat. Freq. in each Bin

scatter(BinCenters, N, 10)              % Histogram Plot
xlabel('Natural Frequency (rad/s)')
ylabel('Amount')
```

Appendix B

Square Lattice Matlab code

```
% Cameron S. Nelson
% Schreyer Honors College Thesis on Graphene

clear all
close all
clc

%                DETERMINATION OF NATURAL FREQUENCIES FOR
%                     SQUARE LATTICE OF CARBON ATOMS


% Size of Lattice
I       = 24;                           % Unit Cells in x-direction
J       = I;                            % Unit Cells in y-direction
n_EOM   = 2*I*J;                        % Number of Equations of Motion

% Mass (kg)
m = 12.0107/6.02214129e23/1000;         % Mass of a Carbon Atom

% Force Constant Parameters for 2D Graphene (N/m) [6]
Phi_r_1 = 365.0;                        % Radial
Phi_ti1 = 245.0;                        % Transverse in-plane
Phi_to1 =  98.2;                        % Transverse out-of-plane

k       = Phi_r_1;                      % Bond Longitudinal Stiffness

% Mass and Stiffness Matrices for Lattice
M       = m*eye(n_EOM);                 % Mass Matrix
S       = zeros(n_EOM);                 % Stiffness Matrix (divided by k)

% Iteration to fill Stiffness Matrix based on Equations of Motion
for a = 0: I: n_EOM-I
% i = 1
        S(a+1, a+1      ) =  2;
        S(a+1, a+2      ) = -1;

% i = 2 to I-1
    for b = 2: 1: I-1
        S(a+b, a+b-1    ) = -1;
        S(a+b, a+b      ) =  2;
        S(a+b, a+b+1    ) = -1;
    end

% i = I
        S(a+I, a+I-1    ) = -1;
        S(a+I, a+I      ) =  2;
end

K       = k*S;                          % Stiffness Matrix
```

```
% Determination of Natural Frequencies
IMK     = inv(M)*K;                     % Inverse of M times K
[V, D]  = eig(IMK);                     % V: Eigenvectors of IMK
                                        % D: Eigenvalues along diagonal

Diag    = ones(1, n_EOM);               % Diagonal to Single-Row Matrix
                                        %   Multiplier
w_n     = (Diag*D).^(1/2);              % Row Matrix of Natural Frequencies

% Natural Frequencies Histogram
width = 1e13;                           % Approximate width of Bins
Bins = floor((max(w_n)-min(w_n))/width);% Number of Bins
Width = (max(w_n)-min(w_n))/Bins;       % Actual width of Bins

v = 0;
BinCenters = zeros(1, Bins);            % Centerpoint of Bins Matrix
for w = min(w_n)+Width/2: Width: max(w_n)-Width/2
    v = v+1;
    BinCenters(1, v) = w;               % Centerpoint for Individual Bin
end

N = hist(w_n, Bins);                    % Number of Nat. Freq. in each Bin

scatter(BinCenters, N, 10)              % Histogram Plot
xlabel('Natural Frequency (rad/s)')
ylabel('Amount')
```

Appendix C

Hexagonal Lattice Matlab code

```
% Cameron S. Nelson
% Schreyer Honors College Thesis on Graphene

clear all
close all
clc

%                DETERMINATION OF NATURAL FREQUENCIES FOR
%                   HEXAGONAL LATTICE OF CARBON ATOMS


% Size of Lattice
I       = 17;                           % Unit Cells in i-direction
J       = I;                            % Unit Cells in j-direction
n_EOM   = 4*I*J-4;                      % Number of Equations of Motion

% Mass (kg)
m = 12.0107/6.02214129e23/1000;         % Mass of a Carbon Atom

% Force Constant Parameters for 2D Graphene (N/m) [6]
Phi_r_1 = 365.0;                        % Radial
Phi_ti1 = 245.0;                        % Transverse in-plane
Phi_to1 =  98.2;                        % Transverse out-of-plane

k       = Phi_r_1;                      % Bond Longitudinal Stiffness

% Mass and Stiffness Matrices for Lattice
M       = m*eye(n_EOM);                 % Mass Matrix
S       = zeros(n_EOM);                 % Stiffness Matrix (divided by k/4)

% Iteration to fill Stiffness Matrix based on Equations of Motion
T       = sqrt(3);                      % Square Root of 3
% i = 1, j = 1
        % AX                            % AY
        S(1,   1          ) =  6;       S(2,   2          ) =  6;
                                      % S(2,   N/A        ) = -4;
        S(1,   5          ) = -3;       S(2,   5          ) =  T;
        S(1,   6          ) =  T;       S(2,   6          ) = -1;
        S(1,   4*I-2+3    ) = -3;       S(2,   4*I-2+3    ) = -T;
        S(1,   4*I-2+4    ) = -T;       S(2,   4*I-2+4    ) = -1;

% i = 1, j = 2 to J-1
    for b = 2: 1: J-1
        g = 4*(b-1)-2;
        % AX                            % AY
        S(g+1, g+1        ) =  6;       S(g+2, g+2        ) =  6;
                                        S(g+2, g+4        ) = -4;
        S(g+1, g+7        ) = -3;       S(g+2, g+7        ) =  T;
        S(g+1, g+8        ) =  T;       S(g+2, g+8        ) = -1;
        S(g+1, g+4*I-4+7  ) = -3;       S(g+2, g+4*I-4+7  ) = -T;
        S(g+1, g+4*I-4+8  ) = -T;       S(g+2, g+4*I-4+8  ) = -1;
        if b == 2
            z = 2;
        else
            z = 0;
```

```
        end
        % BX                                % BY
        S(g+3, g+3        ) =  6;          S(g+4, g+4        ) =  6;
                                           S(g+4, g+2        ) = -4;
        S(g+3, g-2+z      ) =  T;          S(g+4, g-2+z      ) = -1;
        S(g+3, g-3+z      ) = -3;          S(g+4, g-3+z      ) =  T;
       %S(g+3, N/A        ) = -T;         %S(g+4, N/A        ) = -1;
       %S(g+3, N/A        ) = -3;         %S(g+4, N/A        ) = -T;
    end

% i = 1, j = J
        g = 4*(I-1)-2;
        % AX                               % AY
        S(g+1, g+1        ) =  6;          S(g+2, g+2        ) =  6;
                                           S(g+2, g+4        ) = -4;
       %S(g+1, N/A        ) = -3;         %S(g+2, N/A        ) =  T;
       %S(g+1, N/A        ) =  T;         %S(g+2, N/A        ) = -1;
        S(g+1, g+4*I+3    ) = -3;          S(g+2, g+4*I+3    ) = -T;
        S(g+1, g+4*I+4    ) = -T;          S(g+2, g+4*I+4    ) = -1;
        % BX                               % BY
        S(g+3, g+3        ) =  6;          S(g+4, g+4        ) =  6;
                                           S(g+4, g+2        ) = -4;
        S(g+3, g-2        ) =  T;          S(g+4, g-2        ) = -1;
        S(g+3, g-3        ) = -3;          S(g+4, g-3        ) =  T;
       %S(g+3, N/A        ) = -T;         %S(g+4, N/A        ) = -1;
       %S(g+3, N/A        ) = -3;         %S(g+4, N/A        ) = -T;

% i = 2 to I-1, j = 1
    for a = 2: 1: I-1
        g = 4*I*(a-1)-2;
        % AX                               % AY
        S(g+1, g+1        ) =  6;          S(g+2, g+2        ) =  6;
                                           S(g+2, g+4        ) = -4;
        S(g+1, g+7        ) = -3;          S(g+2, g+7        ) =  T;
        S(g+1, g+8        ) =  T;          S(g+2, g+8        ) = -1;
        S(g+1, g+4*I+3    ) = -3;          S(g+2, g+4*I+3    ) = -T;
        S(g+1, g+4*I+4    ) = -T;          S(g+2, g+4*I+4    ) = -1;
        if a == 2
            z = 2;
        else
            z = 0;
        end
        % BX                               % BY
        S(g+3, g+3        ) =  6;          S(g+4, g+4        ) =  6;
                                           S(g+4, g+2        ) = -4;
       %S(g+3, N/A        ) =  T;         %S(g+4, N/A        ) = -1;
       %S(g+3, N/A        ) = -3;         %S(g+4, N/A        ) =  T;
        S(g+3, g-4*I+2+z  ) = -T;          S(g+4, g-4*I+2+z  ) = -1;
        S(g+3, g-4*I+1+z  ) = -3;          S(g+4, g-4*I+1+z  ) = -T;
    end

% i = 2 to I-1, j = 2 to J-1
for a = 2: 1: I-1
    for b = 2: 1: J-1
        g = 4*I*(a-1)+4*(b-1)-2;
        % AX                               % AY
        S(g+1, g+1        ) =  6;          S(g+2, g+2        ) =  6;
                                           S(g+2, g+4        ) = -4;
        S(g+1, g+7        ) = -3;          S(g+2, g+7        ) =  T;
        S(g+1, g+8        ) =  T;          S(g+2, g+8        ) = -1;
        S(g+1, g+4*I+3    ) = -3;          S(g+2, g+4*I+3    ) = -T;
```

```
        S(g+1, g+4*I+4    ) = -T;       S(g+2, g+4*I+4    ) = -1;
        % BX                           % BY
        S(g+3, g+3        ) =  6;       S(g+4, g+4        ) =  6;
                                        S(g+4, g+2        ) = -4;
        S(g+3, g-2        ) =  T;       S(g+4, g-2        ) = -1;
        S(g+3, g-3        ) = -3;       S(g+4, g-3        ) =  T;
        S(g+3, g-4*I+2    ) = -T;       S(g+4, g-4*I+2    ) = -1;
        S(g+3, g-4*I+1    ) = -3;       S(g+4, g-4*I+1    ) = -T;
    end
end

% i = i = 2 to I-1, j = J
    for a = 2: 1: I-1
        g = 4*I*a-6;
        if a == I-1
            z = 2;
        else
            z = 0;
        end
        % AX                           % AY
        S(g+1, g+1        ) =  6;       S(g+2, g+2        ) =  6;
                                        S(g+2, g+4        ) = -4;
       %S(g+1, N/A        ) = -3;      %S(g+2, N/A        ) =  T;
       %S(g+1, N/A        ) =  T;      %S(g+2, N/A        ) = -1;
        S(g+1, g+4*I+3-z  ) = -3;       S(g+2, g+4*I+3-z  ) = -T;
        S(g+1, g+4*I+4-z  ) = -T;       S(g+2, g+4*I+4-z  ) = -1;
        % BX                           % BY
        S(g+3, g+3        ) =  6;       S(g+4, g+4        ) =  6;
                                        S(g+4, g+2        ) = -4;
        S(g+3, g-2        ) =  T;       S(g+4, g-2        ) = -1;
        S(g+3, g-3        ) = -3;       S(g+4, g-3        ) =  T;
        S(g+3, g-4*I+2    ) = -T;       S(g+4, g-4*I+2    ) = -1;
        S(g+3, g-4*I+1    ) = -3;       S(g+4, g-4*I+1    ) = -T;
    end

% i = I, j = 1
        g = n_EOM-4*I+2;
        % AX                           % AY
        S(g+1, g+1        ) =  6;       S(g+2, g+2        ) =  6;
                                        S(g+2, g+4        ) = -4;
        S(g+1, g+7        ) = -3;       S(g+2, g+7        ) =  T;
        S(g+1, g+8        ) =  T;       S(g+2, g+8        ) = -1;
       %S(g+1, g+4*I+3     ) = -3;      %S(g+2, g+4*I+3     ) = -T;
       %S(g+1, g+4*I+4     ) = -T;      %S(g+2, g+4*I+4     ) = -1;
        % BX                           % BY
        S(g+3, g+3        ) =  6;       S(g+4, g+4        ) =  6;
                                        S(g+4, g+2        ) = -4;
       %S(g+3, g-2        ) =  T;      %S(g+4, g-2        ) = -1;
       %S(g+3, g-3        ) = -3;      %S(g+4, g-3        ) =  T;
        S(g+3, g-4*I+2    ) = -T;       S(g+4, g-4*I+2    ) = -1;
        S(g+3, g-4*I+1    ) = -3;       S(g+4, g-4*I+1    ) = -T;

% i = I, j = 2 to J-1
    for b = 2: 1: J-1
        g = n_EOM+4*(-I+b-1)+2;
        if b == J-1
            z = 2;
        else
            z = 0;
        end
        % AX                           % AY
```

```
        S(g+1, g+1        ) =  6;       S(g+2, g+2        ) =  6;
                                        S(g+2, g+4        ) = -4;
        S(g+1, g+7-z      ) = -3;       S(g+2, g+7-z      ) =  T;
        S(g+1, g+8-z      ) =  T;       S(g+2, g+8-z      ) = -1;
       %S(g+1, g+4*I+3    ) = -3;      %S(g+2, g+4*I+3    ) = -T;
       %S(g+1, g+4*I+4    ) = -T;      %S(g+2, g+4*I+4    ) = -1;
        % BX                            % BY
        S(g+3, g+3        ) =  6;       S(g+4, g+4        ) =  6;
                                        S(g+4, g+2        ) = -4;
        S(g+3, g-2        ) =  T;       S(g+4, g-2        ) = -1;
        S(g+3, g-3        ) = -3;       S(g+4, g-3        ) =  T;
        S(g+3, g-4*I+2    ) = -T;       S(g+4, g-4*I+2    ) = -1;
        S(g+3, g-4*I+1    ) = -3;       S(g+4, g-4*I+1    ) = -T;
    end

% i = I, j = J
        g = n_EOM-4;
        % BX                            % BY
        S(g+3, g+3        ) =  6;       S(g+4, g+4        ) =  6;
                                       %S(g+4, g+2        ) = -4;
        S(g+3, g          ) =  T;       S(g+4, g          ) = -1;
        S(g+3, g-1        ) = -3;       S(g+4, g-1        ) =  T;
        S(g+3, g-4*I+4    ) = -T;       S(g+4, g-4*I+4    ) = -1;
        S(g+3, g-4*I+3    ) = -3;       S(g+4, g-4*I+3    ) = -T;

K       = k/4*S;                      % Stiffness Matrix

% Determination of Natural Frequencies
IMK     = inv(M)*K;                   % Inverse of M times K
[V, D]  = eig(IMK);                   % V: Eigenvectors of IMK
                                      % D: Eigenvalues along diagonal

Diag    = ones(1, n_EOM);             % Diagonal to Single-Row Matrix
                                      %   Multiplier
w_n     = (Diag*D).^(1/2);            % Row Matrix of Natural Frequencies

% Natural Frequencies Histogram
width = 1e12;                         % Approximate width of Bins
Bins = floor((max(w_n)-min(w_n))/width);% Number of Bins
Width = (max(w_n)-min(w_n))/Bins;     % Actual width of Bins

v = 0;
BinCenters = zeros(1, Bins);          % Centerpoint of Bins Matrix
for w = min(w_n)+Width/2: Width: max(w_n)-Width/2
    v = v+1;
    BinCenters(1, v) = w;             % Centerpoint for Individual Bin
end

N = hist(w_n, Bins);                  % Number of Nat. Freq. in each Bin

scatter(BinCenters, N, 10)            % Histogram Plot
xlabel('Natural Frequency (rad/s)')
ylabel('Amount')
```

BIBLIOGRAPHY

[1] "Carbon." *Van Nostrand Reinhold Encyclopedia of Chemistry*. New York: 1984.

[2] Jorio, A., R. Saito, G. Dresselhaus, M.S. Dresselhaus. *Raman Spectroscopy in Graphene Related Systems*. Weinheim: Wiley-VCH Verlag GmbH, 2011.

[3] Castro Neto, A.H., F. Guinea, N.M.R. Peres, K.S. Novoselov, A.K. Geim. "The Electronic Properties of Graphene." *Reviews of Modern Physics*. 81. (2009): 109-162.

[4] Castro Neto, A.H., F. Guinea. "Electron-phonon coupling and Raman-spectroscopy in graphene." *Physics Review B*. 75. (2007): 045404.

[5] Saito, R., G. Dresselhaus, M.S. Dresselhaus. *Physical Properties of Carbon Nanotubes*. London: Imperial College Press, 1998.

[6] Jishi, R.A., L. Venkataraman,M.S. Dresselhaus, G. Dresselhaus. "Phonon Modes in Carbon Nanotubules." *Chemistry Physics Letters*. 209.1-2 (1993): 77-82.

[7] Sinha, Alok. *Vibration of Mechanical Systems*. 1st ed. New York: Cambridge University Press, 2010.

[8] Ghosh, Anupama. Private Discussions. Nov 2013.

[9] Feng, Simin. Private Discussions. 11 Feb 2014.

[10] Malard, L.M., M.A. Pimenta, G. Dresselhaus, M.S. Dresselhaus. "Raman Spectroscopy in Graphene." *Physics Reports*. 473. (2009): 51-87.

ACADEMIC VITA

Cameron S. Nelson
3550 E Prospect RD
York, PA 17402
csn5043@psu.edu

EDUCATION

The Pennsylvania State University
M. S. Degree in Mechanical Engineering, graduating May '16

Schreyer Honors College
B. S. Degree in Mechanical Engineering, graduating May '14

Curriculum Highlights:
- 34 total honors credits in Honors Thesis on Graphene (6), M E Intro. to Combustion (3), M E Design Methodology (3), M E Vibration of Mechanical Systems (3), Physics (8), Calculus (8), and Western Music History (3)
- Passed Fundamentals of Engineering exam (EIT) (Oct. '13)

INTERNSHIPS

Exelon, Kennett Square, PA (June to Aug. '13)
Engineering Intern
- Analyzed inspection data for the containment structure tendons at Braidwood Station
- Organized my observations of these tendons into plots, tables, diagrams, a report, and a presentation

Weir American Hydro, York, PA (June to Aug. '12)
Engineering Intern
- 2D and 3D Drafting using NX
- Drafted shafts, hydro turbines, head covers, piping schematics, hardware, assemblies
- Performed blade profile accuracy analyses

EMPLOYMENT

Pennsylvania State University, York, PA (Feb. to Apr. '12)
Tutor
- Mechanical Physics and Calculus.

HONORS SOCIETIES & COMMUNITY ACTIVITIES

- Penn State University Park Orchestra ('13 to '14)
- National Honors Society
- York Youth Symphony Orchestra ('07 to '10)
- Grace Fellowship Church Tech. Team member ('05 to '10)